Hermite Polynomials And Helicoidal Minimal Surfaces

Martin Traizet Matthias Weber

November 1, 2004

Abstract

The main objective of this paper is to construct smooth 1-parameter families of embedded minimal surfaces in euclidean space that are invariant under a screw motion and are asymptotic to the helicoid. Some of these families are significant because they generalize the screw motion invariant helicoid with handles and thus suggest a pathway to the construction of higher genus helicoids. As a byproduct, we are able to relate limits of minimal surface families to the zero-sets of Hermite polynomials.

1 Introduction

Among the embedded periodic minimal surfaces in euclidean space the ones that are invariant under a screw motion (but not under a translation) enjoy the fame of being most inaccessible.

On the other hand, the (known) screw motion invariant helicoids with handles ([1, 3]) have a spectacular limit, the genus one helicoid ([12]), and there is numerical evidence that higher genus helicoids can be obtained as limits of screw motion invariant helicoids with more handles. This paper makes the first step beyond numerical evidence towards an existence proof of a genus g helicoid by proving

Theorem. *There exists, for each $g \geq 1$ and $0 < t < \epsilon$, a family H_g^t of embedded periodic minimal surfaces asymptotic to the helicoid; each family is invariant under vertical screw motions with angle $\pi(1+t)$ and translation π. The quotient surfaces have genus g and two helicoidal ends with winding number $(1+t)/2$.*

This will be a consequence of Theorems 1 and 2, stated in the following section. See also section 3. Heuristically, these surfaces are obtained by gluing helicoids together.

Let's begin with a survey of known results about embedded screw-motion invariant minimal surfaces:

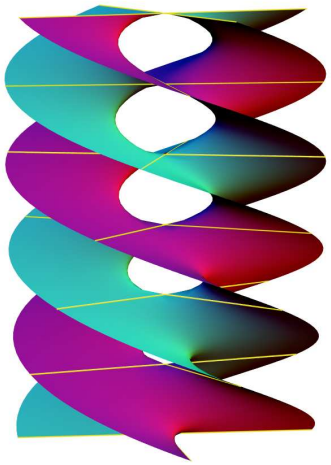

Figure 1: Helicoidal limits of the twisted Karcher-Scherk surfaces.

The first such family of examples was constructed by Karcher in [4], where also the logarithmic differential of the Gauss map is introduced to overcome the difficulty that the Gauss map is not invariant under the screw motion. By pushing the screw motion parameter to its limits, the surfaces degenerate into several helicoidal components ([11]), as illustrated in Figure 1. This suggested to construct the family by gluing two helicoids together. In the language of this paper, the family is obtained using a $(--)$-configuration (which means that we glue two left handed helicoids).

Historically the next family was derived by Hoffman and Karcher, with images made by Wohlrab. They deform translation invariant examples of Fischer and Koch ([9]), and prove the existence and embeddedness using Plateau methods. The Weierstrass representation of these surfaces was discussed in an unpublished Diplom thesis ([5]), where the period problem is not solved, however. Also note that the continuity of the family is not evident from the Hoffman-Karcher construction. We believe that we reproduce the strongly twisted versions of these surfaces by using our $(---)$ configuration, but we haven't proven this.

The third family is related to the genus one helicoid: In ([1, 2]) it is shown that there is an embedded, translation invariant minimal surface asymptotic to the helicoid of genus 1 in the quotient. Numerical experiments [3] suggested that this surface should also exist in a screw motion invariant version. Furthermore, their computer images made it plausible that for increasing screw motion angle, the family would converge to the genus one helicoid.

This latter surface ([1]) is of comparable importance in the theory as the Costa surface: It is the first (and so far the only) example of an embedded minimal surface with a helicoidal end of finite type besides the helicoid itself.

The existence of the family of screw motion invariant helicoids was proven later ([10, 12]) and then used to show that the genus one helicoid as a limit of the family for increasing screw motion angle is indeed embedded.

The motivation for our investigations came from a numerical analysis of the *other* limit for *decreasing* screw motion angle. Computer images indicated that the surfaces would degenerate into three helicoids, two right-handed and one left-handed. This exciting observation suggested that also this family might be constructed by gluing helicoids together. In this paper, we will use the $(+-+)$-configuration for this particular family.

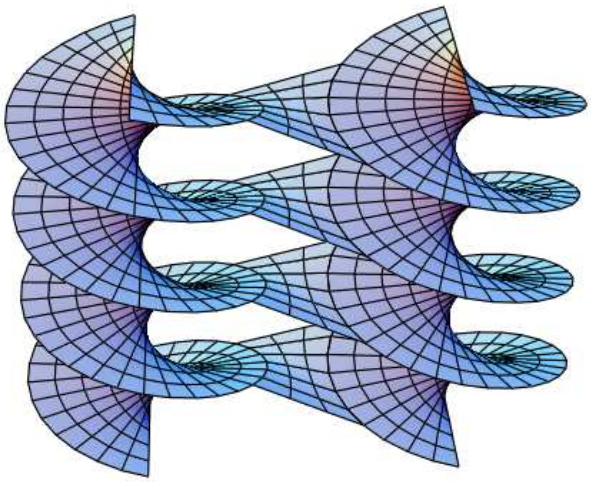

Figure 2: Tentative gluing of two helicoids.

To address this gluing problem, we start near a putative limit configuration, where the helicoids to be glued are given by the positions p_i^0 of their axes as points in the xy-plane, together with a sign $\epsilon_i \in \{\pm 1\}$ at each point, indicating whether the helicoid is left- or right-handed.

It turns out hat this approach leads indeed to a minimal surface family with the desired properties, provided that the points p_i^0 satisfy an explicit set of equations, the balance conditions, to be explained in the next section.

We will limit the discussion to the case that all the p_i^0 lie on the real line, because this leads to an additional symmetry which makes the construction much simpler.

From the configuration data, a space of candidate Riemann surfaces on a fixed topological model surface and Weierstrass data is derived, where the space parameters include the twist parameter t and certain free parameters p_i near p_i^0 and $r_i \geq 0$ that are needed to solve the period problem.

The Weierstrass data are constructed in such a way that as many period conditions as possible are automatically solved. It turns out that one can prescribe the height differential uniquely by solving all period conditions, without any restrictions on the parameters. For the Gauss map, we first define its logarithmic differential. Here one essentially needs to use all the r_i parameters to make the differential integrable to a Gauss map with the right multivaluedness and singularities. This is achieved by a first application of

the implicit function theorem.

Then it remains to solve the period conditions for the first two coordinate differentials. These are transcendental in general, but can be evaluated explicitly in the limit case $t = 0$ and lead there to a set of algebraic equations (called balance equations) in the configuration data p_i. A configuration which solves these balance equations will be called balanced. To apply the implicit function theorem again, we need to require an explicit non-degeneracy condition in terms of the p_i.

We will provide two classes of non-degenerate balanced configurations. The first one leads to surfaces generalizing the Karcher-Scherk surfaces, the second one the screw-motion invariant helicoid. Both classes give rise to new minimal surface families whose quotient surfaces have arbitrarily large genus. The two configurations are explicit in the sense that they are given by the roots of Hermite polynomials. It is a great surprise that limits of minimal surfaces are related to the roots of classical polynomials.

The work in this paper is inspired by [8] where minimal surfaces are constructed by gluing catenoids. The new difficulty in this paper is that the Gauss map is multi-valued, so one more integration step is required. On the other hand, the symmetries greatly simplify the construction, in particular our Riemann surfaces are hyperelliptic. The proof of Theorem 1 in the complex case (namely when the points p_i are not restricted to be real) require the full strength of the arguments in [8].

Below are two figures of the minimal surfaces near the degenerate limit.

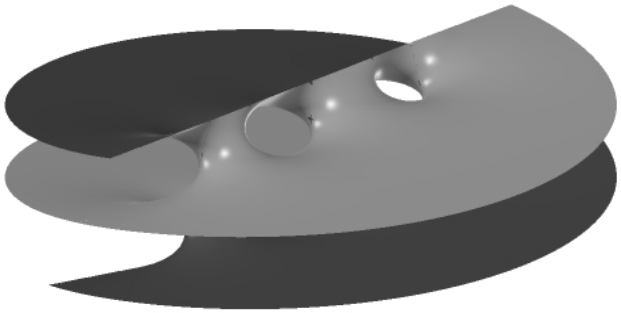

Figure 3: One fundamental piece of numerical solutions to the period problem near the degenerate limit (at $t = 0.05$) for the (+,-,+,-,+) configuration, corresponding to H_2^t.

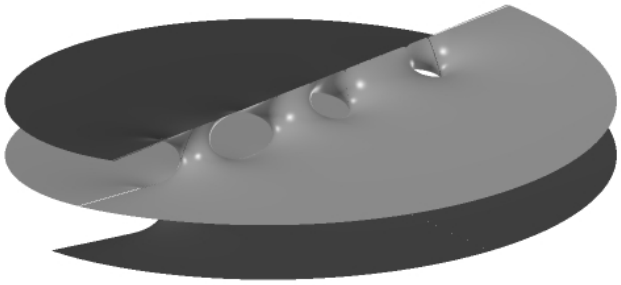

Figure 4: One fundamental piece of numerical solutions to the period problem near the degenerate limit (at $t = 0.05$) for the (+,-,+,-,+,-,+) configuration, corresponding to H_3^t.

Part of this research was done while both authors were visiting M.S.R.I. in Berkeley.

We would like to thank David Hoffman for the invitation and many discussions. We are also grateful to Hermann Karcher and the referee for their suggestions.

We would also like to thank Jim Hoffman for his help in preparing the figures 3 and 4. These images were computed with the program MESH using the explicit Weierstrass data we obtain in this paper. We have to

stress the difference between these true pictures, and our fake rescaled limit pictures. The fact that these pictures look right provides some evidence that the computations in the paper reflect the desired geometry.

2 Main Results

This section states our theorems and introduces the essential notation.

A *configuration* is given by a finite collection of points $p_1, \cdots, p_n$ on the real line, with $p_i < p_{i+1}$. Each point p_i is assigned a *charge* $\varepsilon_i = \pm 1$.

We define the forces $F_1, \ldots, F_n$ by

$$F_i = p_i + \sum_{j \neq i} \frac{\varepsilon_j}{p_i - p_j} \quad .$$

We say the configuration is *balanced* if $F_i = 0$ for all i. We say the configuration is *non-degenerate* if the $n \times n$ matrix $\partial F_i / \partial p_j$ is invertible. Let

$$N = \sum_{i=1}^{n} \varepsilon_i \quad .$$

Theorem 1 *Assume that we are given a configuration which is balanced and non-degenerate. Further assume that $N \neq 0$. Then there exists $\epsilon > 0$ and a smooth 1-parameter family $\{M_t\}_{0<t<\epsilon}$ of embedded minimal surfaces such that:*

1. *the surface M_t is invariant by the vertical screw motion S_t with angle $2\pi t$ about the vertical axis, and translation $(0, 0, 2\pi)$. The quotient M_t / S_t has genus $n - 1$ and two helicoidal ends with winding number $1 + Nt$.*

2. *In a neighborhood of $\frac{1}{\sqrt{t}}(p_i, 0, 0)$, the surface M_t converges to a right or left helicoid of period $(0, 0, 2\pi)$, depending respectively on wether $\varepsilon_i = 1$ or $\varepsilon_i = -1$.*

3. *Let $\mathcal{M}_t$ be the result of rescaling the horizontal part of M_t by $\sqrt{t}$ (the modified surface is not a minimal surface, unless $n = 1$, in which case M_t is a helicoid). Then $\mathcal{M}_t$ converges (as sets) to the surface $\mathcal{M}_0$ defined as follows: consider the multi-valued function*

$$f(z) = \sum_{i=1}^{n} \varepsilon_i \arg(z - p_i) \ , \qquad z \in \mathbb{C} \setminus \{p_1, \cdots, p_n\} \quad .$$

$\mathcal{M}_0$ is the union of the multi-graph of f, the multi-graph of $f + \pi$, and the vertical lines through all points p_i. It is a smooth, complete surface.

This theorem will be proven in section 5. A comment about the different types of limits we consider might be in order. Usually, a minimal surface has no preferred position or size in space, it can be moved and scaled (uniformly). Therefore, when one talks about the (geometric) limit of a family of minimal surfaces, this refers to some normalization of the position of all the surfaces, and different normalizations usually give different geometric limits.

If, however, one ignores the metric structure and considers only the conformal structures of the underlying Riemann surfaces, the limit object is frequently an ungeometric *noded* surface whose components and nodes are responsible for the different geometric limits one can obtain. This second type of limit is the one we are pursuing in this paper.

However, the third part of our Theorem 1 indicated that it might be worthwhile to consider also a third type of limit where one allows for affine renormalizations of the families in the surfaces. In our case, we obtain limits that still have all of the topology of the original surfaces but are much simpler in their formal description. As a drawback we loose minimality, on the other hand the parameterizations are now given by harmonic functions.

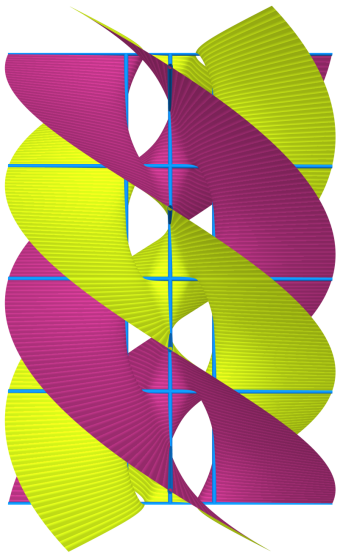

Figure 5: Rescaled limit surface in the $(-,-,-)$ case.

We will show that non-degenerate balanced configurations exist in the following two cases:

Theorem 2 *Let H_n be the Hermite polynomial of degree n. Then the following two configurations are non-degenerate and balanced:*

1. *For each n, let $p_i, \quad i = 1, \ldots, n$ be the zeroes of H_n together with the charges $\epsilon_i = -1$.*

2. *For each $n = 2m + 1$, let $x_i, \quad i = 1, \ldots, m + 1$ be the zeroes of H_{m+1} together with the charges $\epsilon_i = 1$ and let $y_i, \quad i = 1, \ldots, m$ be the zeroes of H_m together with the charges $\epsilon_i = -1$. Let $\{p_i\}$ be the union of the x_i and y_i.*

The two parts of this theorem will be proven in sections 6.4 and 6.5 as corollaries 2 and 3.

3 Relation with known examples

In this section, we explain how the family we construct in the $(+,-,+)$ case is related to the screw motion invariant genus one helicoid, and the $(-,-)$ case is related to the twisted Karcher-Scherk surfaces.

Observe that our surfaces in the $(+,-,+)$ case have genus 2 and not 1. As we shall see, the reason for this is that we construct in fact a branched double cover of the screw motion invariant genus one helicoid, branched over the two points $\infty_{1,2}$ representing the helicoidal ends.

Consider first the second case in Theorem 2, namely $n = 2m + 1$ with alternating charges. Since the configuration is symmetric about the origin, the surfaces M_t have additional symmetries (see the end of section 4) and in particular are invariant by the screw motion $\widetilde{S}_t$ with angle $\pi(1 + t)$ and translation π. Observe that $\widetilde{S}_t \circ \widetilde{S}_t = S_t$. The quotient $M_t/\widetilde{S}_t$ has genus m (see below) and two helicoidal ends with winding number $(1 + t)/2$ each.

In particular, in the $(+,-,+)$ case, $M_t/\widetilde{S}_t$ has genus 1, and two ends of winding number slightly more than $1/2$, as t is a small positive number.

Therefore, this surfaces M_t are screw motion invariant genus one helicoids each, in the same sense as the surfaces constructed by [12]. It is not clear, however, that our surfaces are the same surfaces. To prove this, one should show that the genus one helicoid family in [12] degenerates into three helicoids. The result would then follow, because our use of the implicit function theorem implies that the family is unique near the degenerate limit.

Numerical experiments with the Weierstrass data in [1] suggest that this is indeed the case.

Consider next the $(-,-)$ case (see Figure 1 for an actual minimal surface in the family, and Figure 6 for the rescaled limit). Again, the configuration is symmetric about the origin so the surface is invariant by order 2 rotation about the vertical axis. Composing with S_t, the surface is invariant by the screw motion $\widehat{S}_t$ with angle $\pi + 2\pi t$ and translation 2π. The quotient $M_t/\widehat{S}_t$ has genus 0 (see below) and 4 helicoidal ends with winding number $1/2 - t$ each. We know that $M_t/\widehat{S}_t$ is a twisted Karcher-Scherk surface, see [11].

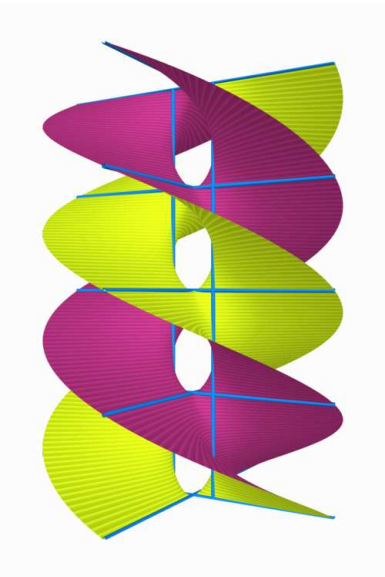

Figure 6: Rescaled limit surface in the $(-,-)$ case. Compare with Figure 1.

The simplest way to compute the genus of M_t in the above quotients is to use the following formula from [6], Theorem 4:

$$C(M) = 2\pi(\chi(M) - W(M)) \quad .$$

Here M is a minimal surface in the quotient of $\mathbb{R}^3$ by a screw motion, $C(M)$ is the total curvature of M, $\chi(M)$ is the Euler characteristic and $W(M)$ is the sum of the winding numbers of the helicoidal ends.

From this formula, we obtain in any case that the total curvature of M_t/S_t is

$$C(M_t/S_t) = 2\pi(2 - 2(n-1) - 2 - 2(1+Nt)) = -4\pi(n+Nt) \quad .$$

Observe that when t is small, the total curvature is close to $-4\pi n$, which is to be expected since we glue n helicoids together.

In the second case of Theorem 2, $C(M_t/\widetilde{S}_t)$ is half of $C(M_t/S_t)$. Clearly this determines the Euler characteristic, hence the genus, of $M_t/\widetilde{S}_t$. We omit the details.

In the first case of Theorem 2, $M_t/\widehat{S}_t$ and M_t/S_t have the same total curvature because $M_t/S_t \circ S_t$ is a double cover of both. Again this determines the genus of $M_t/\widehat{S}_t$.

4 Geometric Model and Weierstrass Representation

In this section, we assume that the surface M_t exists, and we derive informations about its Weierstrass data from its geometrical picture. In the next sections, we will use this information to define all possible candidates for the Weierstrass data, and prove existence of the surface M_t.

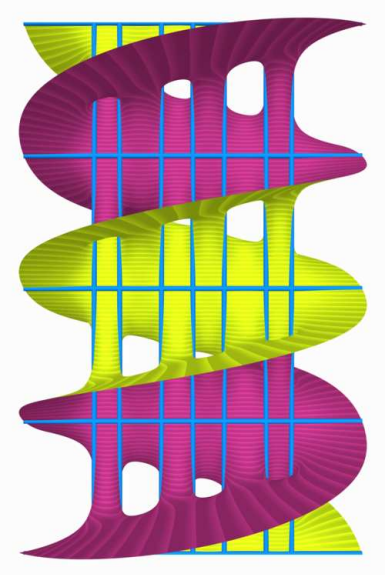

Figure 7: Rescaled limit surface in the $(+,-,+,-,+,-,+)$ case.

It is quite difficult to draw a helicoid. We represent a helicoid by drawing two parallel helices which represent its intersection with a vertical cylinder.

In Figure 8, the reader should imagine that there is a small helicoid inside each cylindrical box (these are not truly cylinders, because the surface is invariant by a screw motion).

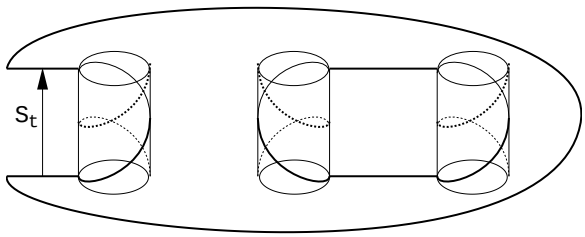

Figure 8: Geometrical model.

Outside of the cylinders, the quotient M_t/S_t has two components. Only one of them is drawn on the picture for clarity. It is bounded by the helices which are drawn as plain curves. The other component is bounded by the helices which are drawn with dots. At infinity, each component is asymptotic to a helicoid.

We now consider the Weierstrass data of the surface. We shall work in the quotient M_t/S_t. From the conformal point of view this is a Riemann surface which we call Σ_t or just Σ. The Gauss map G and height differential dh of M_t satisfy $G \circ S_t = \exp(2\pi\sqrt{-1}t)G$ and $S_t^* dh = dh$. So dh descends to the quotient, but G does not. On the other hand, the logarithmic differential $\omega = dG/G$ satisfy $S_t^*\omega = \omega$, so ω descends to the quotient. Our strategy will be to construct first Σ, dh and ω, and then recover the Gauss map by $G = \exp(\int \omega)$.

Inside each cylinder, the surface is close to a helicoid, so in the quotient, is conformally an annulus close to $\mathbb{C} \setminus \{0\}$. We may call this a helicoidal neck. Outside of the cylinders, each component is conformally equivalent to the complex plane minus small disks centered at $p_1, \cdots, p_n$. So the quotient $\Sigma = M_t/S_t$ is conformally equivalent to two copies of $\mathbb{C}$ connected by n small necks. The compactification $\overline{\Sigma}$ of Σ (obtained by adding the point at infinity in each copy of $\mathbb{C}$) is a compact Riemann surface of genus $n-1$, see Figure 9.

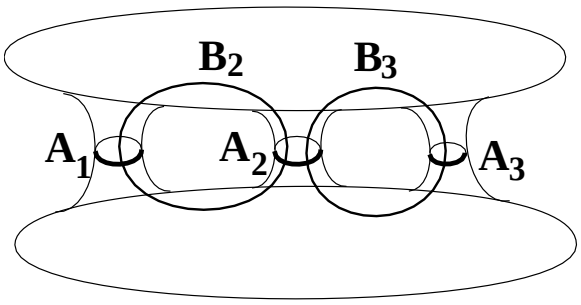

Figure 9: Topological picture of $\overline{\Sigma}$.

We define the following cycles on M_t. Let A_i, $i = 1, \cdots, n$, be the homology class, in the quotient M_t/S_t, of any one of the two helices on the boundary of the cylindrical box corresponding to p_i, oriented so that it climbs up. On the conformal picture of Σ, A_i is a circle which goes around the neck. Note that A_i is not a closed curve on M_t. It is only closed in the quotient. We also define cycles B_i, $i \geq 2$, as on Figure 9, so that $A_2, \cdots, A_n, B_2, \cdots, B_2$ is a homology basis of $\overline{\Sigma}$. The cycles B_i are closed curves on M_t.

Because A_i climbs up, we must require that

$$\mathrm{Re} \int_{A_i} dh = 2\pi \quad .$$

Since the inside of the cylindrical box is close to a helicoid, the variation of $\arg(G)$ along the helix A_i is close to $\pm 2\pi + t$, depending on whether the helicoid is a right or left helicoid, which is determined by ε_i. It should also be equal to $2\pi t$ modulo 2π because the endpoints of A_i are identified by the screw motion S_t. So we require

$$\int_{A_i} dG/G = 2\pi\sqrt{-1}(\varepsilon_i + t) \quad .$$

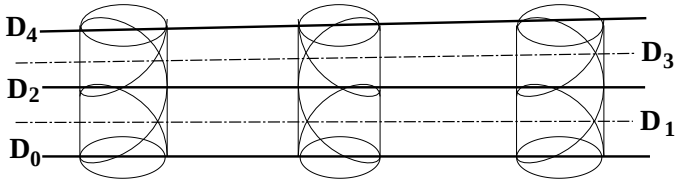

Figure 10: Symmetries of the surface

Finally we describe the symmetries of the surface. We shall construct a minimal surface with the following symmetries (see Figure 10):

Let D_k be the horizontal line defined as the image of the Ox axis by $(S_t)^{k/4}$ (namely, the screw motion with angle $2\pi tk/4$ and vertical translation $2\pi k/4$). For even $k \in \mathbb{Z}$, D_k is a *symmetry line* of M_t, which means that it lies on the surface and the surface is invariant by rotation of order 2 around this line. For odd $k \in \mathbb{Z}$, D_k is a *symmetry axis* of M_t, which means that it is perpendicular to the surface and the surface is invariant by rotation of order 2 around this line.

This translates to the following symmetries of the Weierstrass data of M_t. Let ρ_k be the rotation of order 2 around the line D_k. Then

$$\rho_k^* dh = -\overline{dh} \ , \quad G \circ \rho_k = -e^{\pi\sqrt{-1}kt} G \ , \quad \rho_k^* \omega = \overline{\omega} \ , \quad \text{for even } k \in \mathbb{Z}$$

$$\rho_k^* dh = -dh \ , \quad G \circ \rho_k = \frac{e^{\pi\sqrt{-1}kt}}{G} \ , \quad \rho_k^* \omega = -\omega \ , \quad \text{for odd } k \in \mathbb{Z}$$

In the quotient $\Sigma = M_t/S_t$, for k even, the rotations ρ_k all correspond to the same transformation which we call σ. It is a antiholomorphic involution of Σ. For k odd, the rotations ρ_k all correspond to the same transformation which we call ρ. It is a holomorphic involution of Σ. The quotient Σ/ρ has genus zero, so Σ is a hyperelliptic Riemann surface. The Weierstrass data in the quotient has the symmetries

$$\sigma^* dh = -\overline{dh} \ , \quad \sigma^* \omega = \overline{\omega} \ , \quad \rho^* dh = -dh \ , \quad \rho^* \omega = -\omega \quad .$$

In case the configuration is symmetric about the origin, the vertical axis is a symmetry line of the surface if n is odd, and a symmetry axis if n is even. We will, however, not use this symmetry in the construction, because it does not help very much.

5 Proof of Main Theorem 1

5.1 The Riemann Surface

Let Σ be the hyperelliptic Riemann surface defined by the algebraic equation

$$w^2 = P(z) \quad \text{where} \quad P(z) = \prod_{i=1}^{n} ((z - p_i)^2 + r_i^2) \tag{1}$$

Here $p_1, \cdots, p_n$ are real parameters in a neighborhood of the given configuration, and $r_1, \cdots, r_n$ are positive real numbers in a neighborhood of 0. Together with the screw motion parameter t which will enter the game with the Weierstrass representation, these are all the parameters of the construction.

It is clear that we get isomorphic surfaces by translating the p_i and by scaling the p_i and r_i. This additional freedom does count as parameters and will be removed later on.

We may view Σ as the set of $(z, w) \in \mathbb{C}^2$ satisfying the above equation. We may also view it as the Riemann surface obtained by analytic continuation of the function $\sqrt{P(z)}$. A model for the later is given by the standard "cut and glue" construction: consider two copies of the complex plane, labeled $\mathbb{C}_1$ and $\mathbb{C}_2$. For each $i \leq n$, cut $\mathbb{C}_1$ and $\mathbb{C}_2$ along the segment $[p_i - \sqrt{-1}r_i, p_i + \sqrt{-1}r_i]$. Glue $\mathbb{C}_1$ and $\mathbb{C}_2$ along the cut in the usual way. This is the model we will consider most of the time. The genus of Σ is $n - 1$.

The Riemann surface Σ has all the desired symmetries:

1. Let $\rho : \Sigma \to \Sigma$ be the holomorphic involution which exchanges the point $z \in \mathbb{C}_1$ with the same point $z \in \mathbb{C}_2$ (this is the usual involution of a hyperelliptic Riemann surface). The fixed points of ρ are $p_i \pm \sqrt{-1}r_i$, $i = 1, \cdots, n$.

2. Let $\sigma : \Sigma \to \Sigma$ be the anti-holomorphic involution defined by $z \mapsto \overline{z}$ in $\mathbb{C}_1$ and $\mathbb{C}_2$. The fixed points of σ are the real points of $\mathbb{C}_1$ and $\mathbb{C}_2$.

The two real axes in $\mathbb{C}_1$ and $\mathbb{C}_2$ are visible on the surface in euclidean space as horizontal straight lines, and the involution σ just rotates around these lines by 180°. In our figures, these lines appear as lines in the paper plane.

The vertical slits on the imaginary axes in $\mathbb{C}_1$ and $\mathbb{C}_2$ correspond to the vertical coordinate axis in space, and the the other four half-infinite components on the imaginary axes away from the slits fit together to form horizontal lines on the surface and half way between the other two lines mentioned before. The latter are in are figures perpendicular to the paper plane.

The involution ρ can be seen as a 180° rotation around horizontal lines in space that cut the second ('imaginary') type of lines perpendicularly and do not lie on the surface.

5.1.1 Choice of Cycles

We compactify Σ by adding the points at infinity in $\mathbb{C}_1$ and $\mathbb{C}_2$, which we label ∞_1 and ∞_2. We now define the cycles A_i and B_i in our model for Σ.

Fix some small $\epsilon > 0$. Let A_i, $i = 1, \cdots, n$ be the circle $C(p_i, \epsilon)$ in $\mathbb{C}_1$, oriented with the counter-clockwise orientation if $\varepsilon_i = 1$ and the clockwise orientation if $\varepsilon_i = -1$. A_i is homologous to the circle $C(p_i, \epsilon)$ in $\mathbb{C}_2$ with the opposite orientation.

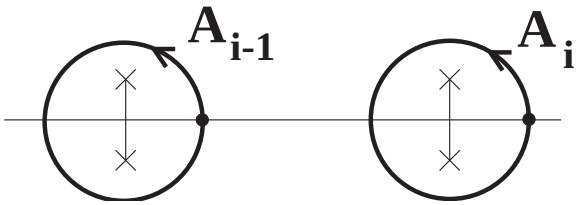

Figure 11: Definition of the cycles A_{i-1} and A_i in the case $\varepsilon_{i-1} = \varepsilon_i = +1$. The vertical segments represent the cuts passing through p_{i-1} and p_i.

Let B_i, $i \geq 2$, be the composition of the following curves: The segment from $p_i + \epsilon$ to $p_{i-1} - \epsilon$, the half circle $z = p_{i-1} - \epsilon \exp(-\sqrt{-1}\varepsilon_{i-1}\theta)$ with $\theta \in [0, \pi]$, the segment from $p_{i-1} + \epsilon$ to $p_i - \epsilon$, and the half circle $z = p_i + \epsilon \exp(\sqrt{-1}\varepsilon_i\theta)$ with $\theta \in [0, \pi]$.

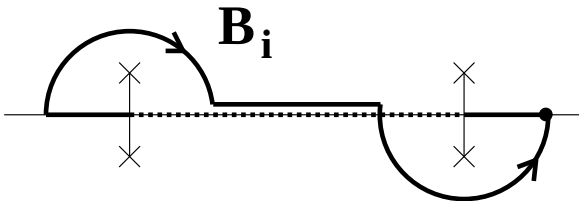

Figure 12: Definition of the cycle B_i in the case $\varepsilon_{i-1} = \varepsilon_i = +1$. The segment drawn with dots lies in $\mathbb{C}_2$ because the path crosses the cuts.

The intersection numbers satisfy $A_i \cdot B_i = \varepsilon_i$ and $A_{i-1} \cdot B_i = -\varepsilon_{i-1}$. The matrix $(A_i \cdot B_j)$, $i, j \geq 2$ is invertible in $SL(n-1, \mathbb{Z})$. It follows that $\{A_2, \cdots, A_n, B_2, \cdots, B_n\}$ is a homology basis of $\overline{\Sigma}$, and holomorphic 1-forms on $\overline{\Sigma}$ are uniquely defined by prescribing their periods along $A_2, \cdots, A_n$.

5.2 The Height Differential

5.2.1 Definition of dh

In order to have helicoidal ends, dh needs simple poles at ∞_1 and ∞_2 with pure imaginary residues, see [6].

By the residue theorem in $\mathbb{C}_1$ and $\mathbb{C}_2$ we have

$$-\sum_{i=1}^{n} \varepsilon_i \int_{A_i} dh = 2\pi\sqrt{-1}\,\mathrm{Res}_{\infty_1} dh = -2\pi\sqrt{-1}\,\mathrm{Res}_{\infty_2} dh \tag{2}$$

It is a standard fact in Riemann surface theory that one can prescribe the poles, the residues, and periods along the cycles $A_2, \ldots, A_n$, with the only condition that the sum of the residues be zero. In our case, because of (2), this is the same as prescribing the periods along *all* cycles $A_1, \cdots, A_n$. Consequently,

Definition 1 *We define dh on $\overline{\Sigma}$ as the unique meromorphic 1-form with two simple poles at ∞_1 and ∞_2, normalized by the period condition*

$$\forall i \geq 1, \qquad \int_{A_i} dh = 2\pi \quad .$$

From (2), the residues of dh at ∞_1 and ∞_2 are then given by

$$\mathrm{Res}_{\infty_1} dh = -\,\mathrm{Res}_{\infty_2} dh = \sqrt{-1}\sum_{i=1}^{n} \varepsilon_i = N\sqrt{-1} \quad .$$

To prove that dh has the required symmetries, observe that $\sigma(A_i) = -A_i$, hence

$$\int_{A_i} \sigma^* dh = \int_{\sigma(A_i)} dh = -\int_{A_i} dh = \overline{-\int_{A_i} dh} \quad .$$

Consequently, the meromorphic forms $\overline{\sigma^* dh}$ and $-dh$ have the same poles, A-periods and residues, so they are equal. In the same way, $\rho(A_i) = -A_i$ implies that $\rho^* dh = -dh$.

5.2.2 B-Periods of dh

Observe that $B_i - \sigma(B_i)$ is homologous to $A_i - A_{i-1}$. From $\sigma^* dh = -\overline{dh}$ we obtain

$$\int_{B_i} dh + \overline{dh} = \int_{B_i} dh - \int_{\sigma(B_i)} dh = \int_{A_i} dh - \int_{A_{i-1}} dh = 0 \quad .$$

Hence $\text{Re} \int_{B_i} dh = 0$.

5.3 Explicit Formula for dh

In this section we obtain an explicit formula for dh. This will only be used to prove Lemma 1 in the next section. It is well known that on the genus $n-1$ hyperelliptic surface $\overline{\Sigma}$, a basis for holomorphic 1-forms is given by $z^j dz/w$ for $0 \leq j \leq n-2$. Here w is defined by the algebraic equation (1).

We fix the sign of w as follows. In a neighborhood of ∞_1 and ∞_2 we have $w^2 \simeq z^{2n}$. We ask that $w \simeq z^n$ in a neighborhood of ∞_1, and consequently, $w \simeq -z^n$ in a neighborhood of ∞_2. Then $z^{n-1}dz/w$ has two simple poles at ∞_1 and ∞_2 with respective residues -1 and $+1$.

From this we can write explicitly

$$dh = -N\sqrt{-1}\frac{z^{n-1}dz}{w} + \sum_{j=0}^{n-2} \alpha_j \frac{z^j dz}{w} \tag{3}$$

The coefficients $\alpha_0, \cdots, \alpha_{n-2}$ are determined by solving the linear equations

$$\int_{A_i} dh = 2\pi \quad 2 \leq i \leq n \quad .$$

The matrix of this linear system is

$$M_{ij} = \int_{A_i} \frac{z^j dz}{w}, \qquad 2 \leq i \leq n, \quad 0 \leq j \leq n-2 \quad .$$

5.3.1 Limit of dh

Recall that Σ, hence dh, are only defined when all r_i are nonzero. We will later need the limit of dh when all $r_i \to 0$.

Lemma 1 *When all r_i go to 0, dh converges uniformly on compact subsets of $\mathbb{C}_1 \setminus \{p_1, \cdots, p_n\}$, to the meromorphic 1-form dh_1 defined by*

$$dh_1 = \sum_{i=1}^{n} \frac{-\sqrt{-1}\varepsilon_i \, dz}{z - p_i} \quad .$$

Moreover, dh (restricted to any compact subset of $\mathbb{C}_1 - \{p_1, \ldots, p_n\}$) extends analytically to $r_i = 0$, (meaning that it extends to an analytic function of all parameters.) A similar statement also holds on $\mathbb{C}_2$.

PROOF: This kind of convergence result is proven in a more general setup in [8] using results by Fay and Masur from algebraic geometry. In our case, we can give a very elementary proof using the formula of the previous section. When all $r_i \to 0$, we have in $\mathbb{C}_1$

$$\lim_{r_i \to 0} w = \prod_{k=1}^{n} (z - p_k) \qquad ,$$

so

$$\lim_{r_i \to 0} M_{ij} = \int_{A_i} \frac{z^j dz}{\prod (z - p_k)} = 2\pi\sqrt{-1} \frac{p_i^j}{\prod_{k \neq i} (p_i - p_k)} \quad .$$

The limit matrix is invertible. This implies that the coefficients α_j extend analytically to $r_i = 0$, so dh converges to a meromorphic differential dh_1 with simple poles at $p_1, \cdots, p_n$ and ∞_1. By continuity

$$\operatorname{Res}_{p_i} dh_1 = \frac{\varepsilon_i}{2\pi\sqrt{-1}} \int_{A_i} dh_1 = -\sqrt{-1}\varepsilon_i \quad .$$

Now a meromorphic 1-form with simple poles on $\mathbb{C} \cup \{\infty\}$ is uniquely determined by its poles and residues. This proves the lemma. Q.E.D.

5.4 The Gauss Map

5.4.1 Definition of the Logarithmic Differential

Recall that we shall first define the logarithmic differential $\omega = dG/G$, and then recover the Gauss map, as a multi-valued function, by $G = \exp(\int \omega)$.

We decide to orient the surface we want to construct so that the Gauss map is infinite at the end ∞_1. From formula (3) dh has $n - 1$ zeroes $q_1, \cdots, q_{n-1}$ in $\mathbb{C}_1$ (see below for a discussion of multiple zeroes). At these zeroes, the Gauss map needs a simple pole, so $\omega = dG/G$ needs a simple pole with residue -1. From the symmetry $\rho^* dh = -dh$, we see that $q_1, \cdots, q_{n-1}$, viewed as points in $\mathbb{C}_2$, are the zeroes of dh in $\mathbb{C}_2$. At these zeroes, the Gauss map needs a simple zero, so ω needs a simple pole with residue $+1$. This motivates

Definition 2 *We define the logarithmic differential ω as the unique meromorphic 1-form on $\overline{\Sigma}$ with simple poles at $q_1, \cdots, q_{n-1}$ in $\mathbb{C}_1$ (resp. $\mathbb{C}_2$) with*

residue -1 *(resp.* $+1$*) and two simple poles at* ∞_1*,* ∞_2*, normalized by the period condition*

$$\forall i \geq 1, \qquad \int_{A_i} \omega = 2\pi\sqrt{-1}(\varepsilon_i + t) \quad .$$

From the residue theorem in $\mathbb{C}_1$, we have

$$-\sum_{i=1}^{n} \varepsilon_i \int_{A_i} \omega = 2\pi\sqrt{-1} \left(\mathrm{Res}_{\infty_1}\omega + \sum_{i=1}^{n-1} \mathrm{Res}_{q_i}\omega \right)$$

which determines the residues at infinity

$$\mathrm{Res}_{\infty_1}\omega = n - 1 - \sum_{i=1}^{n}(\varepsilon_i^2 + t\varepsilon_i) = -1 - tN = -\mathrm{Res}_{\infty_2}\omega \quad .$$

Note that $q_1, \cdots, q_{n-1}$ depend on dh hence on all parameters $p_1, \ldots, p_n$, $r_1, \ldots, r_n$. In case dh has multiple zeroes, the residues of ω should add up. Note that the multiple zeroes of dh do not depend analytically on the parameters. However, ω is a symmetric function of the zeroes, so may be expressed in function of the elementary symmetric functions of the zeroes, which are analytic functions of the parameters. So ω depends analytically on all parameters.

It is straightforward to check that ω has the desired symmetries $\sigma^*\omega = \overline{\omega}$ and $\rho^*\omega = -\omega$.

5.4.2 Limit of the Logarithmic Differential

Similarly as for dh, we have

Lemma 2 *When all* $r_i \to 0$*,* ω *converges on compact subsets of* $\mathbb{C}_1 \backslash \{p_1, \cdots, p_n, q_1, \cdots, q_{n-1}\}$ *to the meromorphic 1-form* ω_1 *on* $\mathbb{C}_1$ *given by*

$$\omega_1 = \sum_{i=1}^{n} \frac{(1 + t\varepsilon_i)dz}{z - p_i} - \sum_{i=1}^{n-1} \frac{dz}{z - q_i} \quad .$$

PROOF: This is proven as Lemma 1. The explicit formula for ω is

$$\omega = (1 + tN)\frac{z^{n-1}dz}{w} + \sum_{j=0}^{n-2} \beta_j \frac{z^j dz}{w} - \sum_{i=1}^{n-1} \frac{w(q_i)\ dz}{(z - q_i)w} \tag{4}$$

where the β_j are determined by solving a linear system of equations coming from the prescribed A-periods. Q.E.D.

5.4.3 B-Periods of ω

In this section we will use the implicit function theorem to find a 1-parameter family of values for the r_i such that all B-periods of ω are zero modulo $2\pi\sqrt{-1}$. This condition on ω is required because $\omega = dG/G$, and we desire G to be single-valued along the B-curves. More precisely:

Proposition 1 *For r_1 small enough, there exists unique $r_2, \cdots, r_n$, depending continuously on r_1 and smoothly on $p_1, \cdots, p_n$ and t, such that*

$$\forall i \geq 2, \quad \int_{B_i} \omega = 0 \bmod 2\pi\sqrt{-1} \quad .$$

PROOF: The imaginary part of $\int_{B_i} \omega$ may be computed using the symmetries: from $\sigma^*\omega = \overline{\omega}$, we have

$$\begin{aligned} \int_{B_i} \omega - \int_{B_i} \overline{\omega} &= \int_{B_i} \omega - \int_{B_i} \sigma^*\omega = \varepsilon_i \int_{A_i} \omega - \varepsilon_{i-1} \int_{A_{i-1}} \omega + \text{residues of } \omega \\ &= 2\pi\sqrt{-1}\varepsilon_i(1+t\varepsilon_i) - 2\pi\sqrt{-1}\varepsilon_{i-1}(1+t\varepsilon_{i-1}) \bmod 2\pi\sqrt{-1} \\ &= 0 \bmod 2\pi\sqrt{-1} \end{aligned}$$

Hence $\text{Im} \int_{B_i} \omega = 0 \bmod 2\pi$. Note that we may have to perturb the curve B_i to avoid possible poles of ω on the real axes, which is why there might be residues in the first line of the computation.

To compute the real part, we need the following lemma:

Lemma 3 *Fix some base point z_0 in $\mathbb{C}_1$. Then*

$$\int_{z_0}^{p_i} \omega = (1+t\varepsilon_i)\log r_i + f(p_1, \cdots, p_n, r_1, \cdots, r_n, t) \quad .$$

where f is an analytic functions of its arguments, the variables $r_1, \cdots, r_n$ being in a neighborhood of 0 and $p_1, \cdots, p_n$ in a neighborhood of the given configuration. (It is understood that the path of integration avoids all other cuts and all poles of ω).

We postpone the proof of the lemma until the proof of the proposition is complete.

Using the symmetry $\rho^*\omega = -\omega$, Lemma 3 implies that

$$\int_{B_i} \omega = 2(1+t\varepsilon_i)\log r_i - 2(1+t\varepsilon_{i-1})\log r_{i-1} + f(p_1, \cdots, p_n, r_1, \cdots, r_n, t)$$

for some analytic function f. We define the renormalized period of ω as

$$\mathcal{F}_i = \frac{1}{\log r_i} \operatorname{Re} \int_{B_i} \omega \quad .$$

We need to solve the equation $\mathcal{F}_i = 0$, $2 \leq i \leq n$. The function $\mathcal{F}_i$ extends continuously to $r_i = 0$, but not smoothly (not even C^1). To solve this problem, write

$$r_i = \exp\left(\frac{-s_i}{\tau^2}\right) \quad \text{with } s_1 = 1 \text{ and } s_i > 0 \quad .$$

Recall that we have fixed a small $r_1 > 0$ which determines τ as a small number near 0. Then

$$\mathcal{F}_i = -2s_i(1 + t\varepsilon_i) + 2s_{i-1}(1 + t\varepsilon_{i-1}) + \tau^2 f(p_1, \cdots, p_n, s_2, \cdots, s_n, \tau)$$

for some other smooth function f. Thus $\mathcal{F}_i$, as a function of τ, $s_2, \cdots, s_n$ and all other parameters, extends smoothly to $\tau = 0$, with

$$\mathcal{F}_i|_{\tau=0} = -2s_i(1 + t\varepsilon_i) + 2s_{i-1}(1 + t\varepsilon_{i-1}) \quad .$$

Solving $\mathcal{F}_i = 0$ when $\tau = 0$ determines $s_2, \cdots, s_n$. The partial differential of $(\mathcal{F}_2, \cdots, \mathcal{F}_n)$ with respect to $(s_2, \cdots, s_n)$ is an isomorphism. We conclude using the implicit function theorem. Q.E.D.

Important note. The real parameter τ introduced in the proof will serve as an auxiliary family parameter from now on. We will later determine t as a function of τ. Also observe that we have normalized the situation so that $s_1 = 1$.

PROOF: (of the lemma) This kind of result is proved in a more general setup in [8]. Here is a simple proof using the explicit formula (4) for ω.

Fix some small $\epsilon > 0$. The integral from z_0 to $p_i + \epsilon$ is an analytic function of all parameters because the path from z_0 to $p_i + \epsilon$ may be chosen inside a compact subset where Lemma 2 applies. Note that the integral of ω depends on the homotopy class of the path of integration, but the integrals on two different paths differ by some $\int_{A_j} \omega$ or $2\pi\sqrt{-1}\operatorname{Res}\omega$. So changing the homotopy class amounts to change the function f.

In a neighborhood of p_i, we may write, by formula (4)

$$\omega = \frac{f(u)\, du}{\sqrt{u^2 + r^2}} \quad \text{where } u = z - p_i \text{ and } r = r_i \qquad ,$$

where f is a holomorphic function on $|u| < \varepsilon$, depending analytically on all parameters. Then we make the change of variable

$$v = \sqrt{u^2 + r^2} + u \quad \Rightarrow \frac{dv}{v} = \frac{du}{\sqrt{u^2 + r^2}}, \quad u = \frac{v^2 - r^2}{2v} \quad .$$

This gives

$$\omega = F\left(v, \frac{r^2}{v}\right) \frac{dv}{v}$$

for some holomorphic function F. We then expand

$$F(x, y) = \sum_{n,m \geq 0} c_{nm} x^n y^m \quad ,$$

where the coefficients c_{nm} depend analytically on all parameters. This gives

$$\omega = \sum_{n,m \geq 0} c_{nm} v^{n-m-1} r^{2m} dv$$

$$\int_{A_i} \omega = 2\pi\sqrt{-1}\varepsilon_i \sum_{n \geq 0} c_{nn} r^{2n}$$

$$\begin{aligned}
\int_{z=p_i+\epsilon}^{p_i} \omega &= \int_{v=\sqrt{\epsilon^2+r^2}+\epsilon}^{r} \sum c_{nm} v^{n-m-1} r^{2m} dv \\
&= \sum_{n \geq 0} c_{nn} r^{2n} \log \frac{r}{\sqrt{\epsilon^2 + r^2} + \epsilon} \\
&+ \sum_{n \neq m} \frac{c_{nm}}{n-m} \left(r^{n+m} - r^{2m} (\sqrt{\epsilon^2 + r^2} + \epsilon)^{n-m} \right) \\
&= \frac{\varepsilon_i}{2\pi\sqrt{-1}} \int_{A_i} \log r + \text{analytic terms} \quad .
\end{aligned}$$

This proves the lemma. Q.E.D.

5.4.4 Normalization of the Gauss Map

We fix a base point $z_0 \in \mathbb{C}_1$, such that z_0 is real and $z_0 < p_1$.

Definition 3 *Let*

$$G(z) = \Lambda\sqrt{-1}\exp\left(\int_{z_0}^{z}\omega\right), \qquad z \in \Sigma \quad ,$$

where the real constant Λ *is chosen so that* $|G| = 1$ *at the point* $p_1 + \sqrt{-1}r_1$ *of* Σ *(which is a fixed point of* ρ*). This defines a multi-valued meromorphic function* G *on* Σ*. It has the following multivaluation: if* γ *is any cycle on* Σ*, then analytic continuation of* G *along* γ *multiplies its value by* $\exp(2\pi\sqrt{-1}kt)$ *where* $k \in \mathbb{Z}$ *is defined by* $\mathrm{Re}\int_\gamma dh = 2\pi k$*.*

It is straightforward to check that the Gauss map has all the desired symmetries. The constant Λ depends on all parameters. Using Lemma 3, we have

$$\begin{aligned} 1 &= |G(p_1 + \sqrt{-1}r_1)| = \Lambda\exp(\,\mathrm{Re}\int_{z_0}^{p_1+\sqrt{-1}r_1}\omega) \\ &= \Lambda\exp((1+t\varepsilon_1)\log r_1 + \text{analytic}) \end{aligned}$$

which gives the estimate

$$\Lambda = \frac{\mathcal{O}(1)}{r_1^{1+t\varepsilon_1}} \tag{5}$$

where $\mathcal{O}(1)$ means a bounded analytic function of the parameters whose inverse is also bounded.

5.4.5 Limit of the Gauss Map

Using Lemma 2 we obtain:

Lemma 4 *On compact subsets of* $\mathbb{C}_1 \setminus \{p_1, \cdots, p_n, q_1, \cdots, q_{n-1}\}$ *we have*

$$G \sim \Lambda\sqrt{-1}\frac{G_1(z)}{G_1(z_0)} \quad \textit{when } \tau \to 0$$

where

$$G_1(z) = \frac{\prod_{i=1}^{n}(z-p_i)^{1+t\varepsilon_i}}{\prod_{i=1}^{n-1}(z-q_i)} \quad .$$

Note that both G and G_1 are multi-valued, but they have the same multi-valuation, so the above statement makes sense (provided we consider the analytic continuation of G and G_1 along the same path).

When $t = 0$, both G and G_1 are single-valued. Also in this case G_1 has the same zeroes and poles as the function dz/dh_1 (where dh_1 is the limit of dh) so they are proportional. This gives (comparing the values at z_0)

$$G \sim c_0 \Lambda \frac{dz}{dh_1} \quad \text{where } c_0 = \sum_{i=1}^{n} \frac{\varepsilon_i}{z_0 - p_i} \quad .$$

5.5 The Period Problem

Let

$$\mu = \frac{1}{2}\left(\overline{G^{-1}dh} - Gdh\right) = dx_1 + i\, dx_2.$$

Note that μ is multi-valued so its integral on a closed curve is not homology invariant.

Let C_i, $i \geq 2$ be the composition of the following paths in $\mathbb{C}_1$: the half circle $z = p_i + \epsilon \exp(\sqrt{-1}\varepsilon_i \theta)$ with $\theta \in [0, \pi]$, the segment from $p_i - \epsilon$ to $p_{i-1} + \epsilon$, the circle $z = p_i + \epsilon \exp(-\sqrt{-1}\varepsilon_{i-1}\theta)$ with $\theta \in [0, 2\pi]$, the segment from $p_{i-1} + \epsilon$ to $p_i - \epsilon$, and the half circle $z = p_i - \epsilon \exp(\sqrt{-1}\varepsilon_i \theta)$ with $\theta \in [0, \pi]$. The point is that C_i is homologous to $A_i - A_{i-1}$.

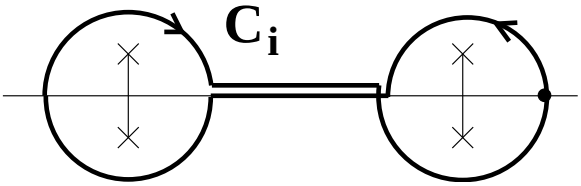

Figure 13: Definition of the cycle C_i in the case $\varepsilon_{i-1} = \varepsilon_i = 1$. The vertical segments represent the cuts passing through p_{i-1} and p_i.

The curves B_i and C_i are meant to be closed curves on M_t, because in our topological model of the surface (see Figure 9), the C_i encircle two helicoidal necks in such an orientation so that they stay on one sheet.

Therefore, we have to require:

$$\forall i \geq 2, \qquad \int_{B_i} \mu = 0, \qquad \int_{C_i} \mu = 0 \tag{6}$$

This is the period problem. Note that multiplying G by $e^{i\theta}$ multiplies μ by the same number, so does not change the fact that the periods are zero. Therefore we may assume that the argument of G is $\pi/2$ at the starting point of B_i and C_i, namely at the point $p_i + \epsilon$.

Also, the Gauss map is single valued on the curves B_i and C_i. So the period problem above is homology invariant — the periods are not homology invariant but the fact that they vanish is invariant.

The following proposition shows that (6) is the only equation we have to solve:

Proposition 2 *Assume that equation (6) is satisfied. Then there exists a screw motion S_t with angle $2\pi t$ and translation part $(0, 0, 2\pi)$ such that* $\mathrm{Re} \int_{z_0}^{z} \phi$ *is well defined modulo S_t, where $\phi = (\phi_1, \phi_2, \phi_3)$ are the three components of the Weierstrass formula.*

PROOF: If γ is an element of the fundamental group $\pi_1(\Sigma, z_0)$, then analytic continuation of the Gauss map along γ multiplies its value by $\exp(2\pi\sqrt{-1}kt)$ where $k \in \mathbb{Z}$ is defined by $\mathrm{Re} \int_\gamma dh = 2\pi k$. So if δ is a path starting at z_0, we have

$$\int_{\gamma * \delta} \mu = \int_\gamma \mu + \exp(2\pi\sqrt{-1}kt) \int_\delta \mu \qquad ,$$

where $*$ denotes composition of paths. Now let $\widehat{A}_i$, $\widehat{B}_i$ be elements of $\pi_1(\Sigma, z_0)$ homologous to A_i and B_i. From (6) we have

$$0 = \int_{\widehat{A}_i * \widehat{A}_{i-1}^{-1}} \mu = \int_{\widehat{A}_i} \mu - \int_{\widehat{A}_{i-1}} \mu \quad .$$

Let $\xi = \int_{\widehat{A}_i} \mu$, independant of i. We have

$$\int_{\widehat{A}_i * \delta} \mu = \xi + \exp(2\pi\sqrt{-1}t) \int_\delta \mu = R_t \left(\int_\delta \mu \right)$$

$$\int_{\widehat{B}_i * \delta} \mu = \int_\delta \mu \qquad ,$$

where R_t is the rotation $R_t(z) = \xi + \exp(2\pi\sqrt{-1}t)z$. Since the fundamental group $\pi_1(\Sigma, z_0)$ is generated by $\widehat{A}_1, \cdots, \widehat{A}_n, \widehat{B}_2, \cdots, \widehat{B}_n$, we obtain by induction

$$\int_{\gamma * \delta} \mu = R_t^k \left(\int_\delta \mu \right), \qquad \mathrm{Re} \int_{\gamma * \delta} dh = 2\pi k + \mathrm{Re} \int_\delta dh \quad .$$

Let S_t be the screw motion with rotation part R_t and translation part $(0, 0, 2\pi)$. The proposition follows. Q.E.D.

5.5.1 Reduction of the period problem

Using the symmetries we prove:

Proposition 3 *The periods satisfy, for each $i \geq 2$,*

$$\mathrm{Re} \int_{C_i} \mu = 0 \tag{7}$$

$$\mathrm{Im} \int_{B_i} \mu = \frac{1}{2} \mathrm{Im} \int_{C_i} \mu \tag{8}$$

$$\mathrm{Re} \left(e^{\pi\sqrt{-1}t/2} \int_{B_i} \mu \right) = 0 \tag{9}$$

Consequently, the period problem is equivalent to (provided $t < 1$)

$$\mathrm{Im} \int_{C_i} \mu = 0 \tag{10}$$

PROOF: Recall that G is single-valued on B_i and C_i and we assumed that $\arg(G) = \pi/2$ at the point $p_i + \epsilon$ which is fixed by σ. From $\sigma^*\omega = \overline{\omega}$ we obtain $\sigma^* G = -\overline{G}$. An easy computation gives $\sigma^*\mu = \overline{\mu}$. Since $\sigma(C_i) = -C_i$,

$$\int_{C_i} \mu = \int_{\sigma(C_i)} \sigma^*\mu = -\int_{C_i} \overline{\mu}$$

which proves (7). Since $\sigma(B_i)^{-1} * B_i$ is homotopic to C_i,

$$\int_{B_i} \mu - \int_{B_i} \overline{\mu} = \int_{C_i} \mu$$

which proves (8) (and also (7) again). To prove (9), we use the symmetry ρ. The Gauss map satisfies $\rho^* G = e^{\pi\sqrt{-1}t}/G$. An elementary computation gives $\rho^*\mu = e^{\pi\sqrt{-1}t}\overline{\mu}$. Since $\rho(B_i)$ is homologous to $-B_i$ this gives

$$\int_{B_i} \mu = -e^{\pi\sqrt{-1}t} \int_{B_i} \overline{\mu}$$

from which we obtain (9). Q.E.D.

5.5.2 Solution of the period problem

To solve the period problem we compute the asymptotics of $\int_{C_i} \mu$ when $\tau \to 0$. We will later fix the dependence of t in function of τ. Here we only need that t will be a smooth function of τ and $t = 0$ when $\tau = 0$. We first compute, using Lemmas 1 and 4,

$$\lim_{\tau\to 0} \Lambda \int_{C_i} G^{-1} dh = \int_{C_i} \frac{1}{c_0} \frac{dh_1^2}{dz} = \frac{2\pi\sqrt{-1}}{c_0} \left(\varepsilon_i \operatorname{Res}_{p_i} dh_1^2 - \varepsilon_{i-1} \operatorname{Res}_{p_{i-1}} dh_1^2 \right)$$

$$\begin{aligned}
\operatorname{Res}_{p_i} dh_1^2 &= \operatorname{Res}_{p_i} \left(\sum_{j=1}^{n} \frac{-\sqrt{-1}\varepsilon_j}{z - p_j} \right)^2 \\
&= -\operatorname{Res}_{p_i} \left(\frac{1}{(z-p_i)^2} + \frac{2}{z-p_i} \sum_{j\neq i} \frac{\varepsilon_i \varepsilon_j}{z-p_j} + \sum_{j,k\neq i} \frac{\varepsilon_j \varepsilon_k}{(z-p_j)(z-p_k)} \right) \\
&= -2 \sum_{j\neq i} \frac{\varepsilon_i \varepsilon_j}{p_i - p_j} \quad .
\end{aligned}$$

To compute the limit of $\Lambda \int_{C_i} G dh$, we want to use a path homologous to C_i. The problem is that the integrand is multi-valued so the integral is not homology invariant. We solve this problem as follows. Let $\psi(z) = (z-p_i)^{-t\varepsilon_i}(z-p_{i-1})^{-t\varepsilon_{i-1}}$. The function ψG is single-valued on A_i and A_{i-1}. Since C_i is homologous to $A_i - A_{i-1}$, we have

$$\int_{C_i} \psi G dh = \int_{A_i} \psi G dh - \int_{A_{i-1}} \psi G dh \quad .$$

Since $\rho(A_i)$ is homologous to $-A_i$, we have

$$\int_{A_i} \psi G dh = -\int_{\rho(A_i)} \psi G dh = -\int_{A_i} \psi \rho^*(G dh) \xrightarrow{\tau\to 0} \int_{A_i} G^{-1} dh \quad .$$

So

$$\lim_{\tau\to 0} \Lambda \int_{C_i} \psi G dh = \lim_{\tau\to 0} \Lambda \int_{C_i} G^{-1} dh$$

which we have already computed above. We compute the remaining term

$$\begin{aligned}
\lim_{\tau\to 0} \Lambda \int_{C_i} (1-\psi) G dh &= \lim_{\tau\to 0} -\Lambda t \int_{C_i} G dh \frac{\left((z-p_i)^{-\varepsilon_i}(z-p_{i-1})^{-\varepsilon_{i-1}}\right)^t - 1}{t} \\
&= \left(\lim_{\tau\to 0} -\Lambda^2 t \right) c_0 \int_{C_i} \log\left((z-p_i)^{-\varepsilon_i}(z-p_{i-1})^{-\varepsilon_{i-1}} \right)
\end{aligned}$$

where we have used that $\lim_{t\to 0} \dfrac{z^t-1}{t} = \log z$. It is an elementary exercise to compute

$$\int_{C_i} -\varepsilon_i \log(z-p_i) - \varepsilon_{i-1}\log(z-p_{i-1}) = 2\pi\sqrt{-1}(p_i - p_{i-1}) \quad .$$

The main Ansatz of the paper is that we now choose t as a function of τ so that the limit of $\Lambda^2 t$ when $\tau \to 0$ exists and is nonzero. The actual value of the limit is a matter of normalization of the scaling of the configuration. (It looks like we are loosing one parameter here, but this is not the case: choosing t in function of τ turns out to be a way to normalize scaling in $\mathbb{C}_1$.) It is convenient to choose

$$\lim_{\tau\to 0} \Lambda^2 t = \frac{4}{{c_0}^2} \quad .$$

That this is possible follows easily from the estimate (5), which gives that t is of the order of r_1^2. This implies, collecting all terms,

$$\lim_{\tau\to 0} \Lambda \int_{C_i} \mu = \frac{4\pi\sqrt{-1}}{c_0}\left(\sum_{j\neq i} \frac{\varepsilon_j}{p_i - p_j} - \sum_{j\neq i-1} \frac{\varepsilon_j}{p_{i-1}-p_j} + p_i - p_{i-1}\right) \quad .$$

Define the renormalized period $\mathcal{F}_i$, $i \geq 2$, by

$$\mathcal{F}_i(\tau, p_1, \cdots, p_n) = \frac{c_0\Lambda}{4\pi} \operatorname{Im}\left(\int_{C_i} \mu\right) \quad .$$

It follows from the above computations that $\mathcal{F}_i$ extends smoothly to $\tau = 0$. To see this, simply observe that all integrals are computed on paths staying at distance at least $\epsilon/2$ from the cuts, so Lemma 1 applies. Moreover, we have

$$\mathcal{F}_i|_{\tau=0} = F_i - F_{i-1} \quad .$$

So when $\tau = 0$, the period problem is equivalent to $F_i =$ constant, independant of i. By translation of $p_1, \ldots, p_n$, we may assume that the constant is zero. This gives the balancing condition $F_i = 0$ stated in the introduction. In fact choosing the constant equal to zero is only a way to normalize the translation of the configuration. It is straightforward to see that the nondegeneracy condition stated in the introduction is equivalent to the fact that the partial differential of $(\mathcal{F}_2, \cdots, \mathcal{F}_n)$ with respect to $(p_1, \cdots, p_n)$ is surjective.

We apply the implicit function theorem at the point $\tau = 0$ and $p_1, \cdots, p_n$ equal to the given configuration to obtain:

Proposition 4 *For τ in a neighborhood of 0, there exists smooth functions $p_1(\tau), \cdots, p_n(\tau)$, such that $\mathcal{F}_i(\tau, p_1(\tau), \cdots, p_n(\tau)) = 0$ so the period problem is solved.*

5.6 Embeddedness

Let $X : \Sigma \to \mathbb{R}^3$ be the minimal immersion given by the Weierstrass data we have constructed. It is multi-valued but well defined modulo the screw motion S_t. In this section, we prove that its image is embedded and actually has all the desired geometric properties built into its definition.

From our choice of t we have $c_0\Lambda \sim 2/\sqrt{t}$ when $\tau \to 0$. Fix some $\epsilon > 0$ and let K_1 be the compact subset of $\mathbb{C}_1$ defined by $|z - p_i| > \epsilon \ \forall i$. From Lemma1 and Lemma 4, we have on K_1

$$dX_1 + \sqrt{-1}dX_2 = \mu \sim \frac{-c_0\Lambda}{2}dz \sim \frac{-dz}{\sqrt{t}} \quad \text{when } \tau \to 0$$

$$\lim_{\tau\to 0} X_3(z) = \ \mathrm{Re} \int_{z_0}^{z} \sum_{i=1}^{n} \frac{-\sqrt{-1}\varepsilon_i}{z - p_i} dz = \sum_{i=1}^{n} \varepsilon_i \arg\left(\frac{z - p_i}{z_0 - p_i}\right) \quad .$$

Hence, up to translation and scaling the horizontal part by $-\sqrt{t}$, the image of K_1 converges to the graph of the multi-valued function

$$f(z) = \sum_{i=1}^{n} \varepsilon_i \arg(z - p_i) \qquad z \in \mathbb{C} \setminus \{p_1 \cdots, p_n\} \quad .$$

From the symmetries, the image of $K_2 = \rho(K_1)$ converges to the same graph translated vertically by π. Note that these two multigraphs may be completed into a smooth surface by adding the vertical lines through each p_i. This proves that the image of $K_1 \cup K_2$ is embedded for τ small enough.

We now consider the image of the domain in $\mathbb{C}_1$ defined by $|z - p_i| < cr_i$ and $\mathrm{Im}\,(z) > 0$ for some fixed i and $c \gg 1$. Write

$$r = r_i \qquad z = p_i + r\zeta \qquad \xi = \sqrt{1 + \zeta^2} + \zeta \quad .$$

Note that ξ is a conformal representation of the domain $|\zeta| < c$ in $\mathbb{C}_1$ minus the cut. We obtain,

$$\lim_{\tau\to 0} dh = -\sqrt{-1}\varepsilon_i \frac{d\xi}{\xi} \qquad \lim_{\tau\to 0} \omega = \frac{d\xi}{\xi} \quad .$$

with uniform convergence on $|\zeta| < c$. Since $|G| = 1$ at the point $z = p_i + \sqrt{-1}r_i$, namely $\xi = \sqrt{-1}$, this gives

$$\lim_{\tau \to 0} G = e^{i\theta} \frac{d\xi}{\xi} \quad .$$

This is the Weierstrass data of a right or left helicoid, depending on $\varepsilon_i = 1$ or $\varepsilon_i = -1$. This proves that the image of $|z - p_i| < cr_i$ converges to a piece of a helicoid, so is embedded.

It remains to understand what happens in the region $cr_i < |z - p_i| < \epsilon$. First observe that from the proof of Lemma 3,

$$|G(z)| = \left(\frac{|z - p_i|}{r} \right)^{1 + t\varepsilon_i} \times \mathcal{O}(1) \qquad ,$$

so provided c is large enough, we have $|G| > 1$ in the domain under consideration. This implies that the map (X_1, X_2) is regular.

Consider the domain in $\mathbb{C}_1$ defined by $cr_i < |z - p_i| < \epsilon$ and $\mathrm{Im}\,(z) > 0$. The image Ω of this domain is bounded by two straight line segments and two curves close to helices, see Figure 14. Let f be the projection onto the horizontal plane and D be the domain in the plane bounded by $f(\partial\Omega)$. Then f is a local homeomorphism, D is simply-connected and $f : \partial\Omega \to \partial D$ is a homeomorphism. This implies that $f : \Omega \to D$ is a homeomorphism, so that Ω is a graph over D hence embedded. (Proof: this is a topological issue, so we may assume by uniformization that D is the unit disk. Then $||f||$ attains its maximum on the boundary of Ω because f is a local homeomorphism. Since $||f|| = 1$ on the boundary, we have $||f|| < 1$ in Ω so $f(\Omega) \subset D$. Since f is proper, this implies that $f : \Omega \to D$ is a covering map. Since there is only one sheet in a neighborhood of the boundary, f is a homeomorphism.)

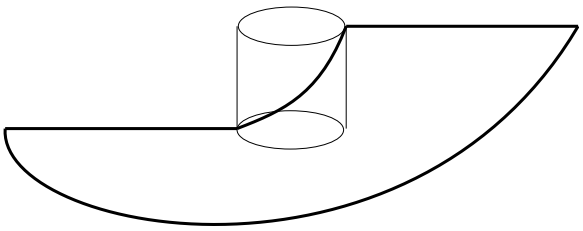

Figure 14: Ω is a graph.

This implies that the whole surface is embedded. We now prove that the convergence to the multigraph holds everywhere. Consider the multigraph

in a neighborhood of p_i and scale its horizontal part by $1/\sqrt{t}$. Call it the rescaled multigraph. Given some $\alpha > 0$, we may choose $\epsilon > 0$ so that the rescaled multigraph is at vertical distance less than α from the piece of helicoid bounded by the two straight line segments. Then for τ small enough, both boundary curves are at vertical distance less than α from the helicoid. By the maximum principle for minimal graphs, Ω is at vertical distance less than α from the helicoid, so at distance less than 2α from the rescaled multigraph. This remains true when we scale the horizontal part by $\sqrt{t}$, and proves that the whole surface, after rescaling, converges to the multigraph as a set.

6 Examples of Non-degenerate Balanced Configurations

In this section, we will prove the existence of two families of non-degenerate balance configurations with arbitrarily many points from Theorem 2.

Both families are intimately related to the zeroes of Hermite polynomials.

6.1 Review of Hermite polynomials

The Hermite polynomials $H_n(x)$ are polynomials of degree n which can be conveniently defined as

$$H_n(x) = e^{x^2}(-1)^n \left(\frac{d}{dx}\right)^n e^{-x^2} \tag{11}$$

The first few are

$$\begin{aligned} H_0(x) &= 1 \\ H_1(x) &= 2x \\ H_2(x) &= 4x^2 - 2 \\ H_3(x) &= 8x^3 - 12x \end{aligned}$$

They satisfy the recurrence relation

$$H_{n+1}(x) = 2xH_n(x) - 2nH_{n-1}(x) \tag{12}$$

For our purposes important is the following differential equation:

$$H_n''(x) - 2xH_n'(x) + 2nH_n(x) = 0 \tag{13}$$

We will also need

$$H_n'(x) = 2nH_{n-1}(x) \tag{14}$$

Assuming (14), differentiating (11) proves (12), and differentiating once further and using (14) for $n+1$ instead of n again shows (13).

We refer to [7] for the proofs of these formulas as well as for a proof of Proposition 5 below.

6.2 Relation Between the Roots

In this section, we use a well-known formula for polynomials with isolated roots together with the differential equation of the Hermite polynomials to prove a key identity for their roots.

Proposition 5 *Let*

$$P(x) = c\prod_{i=1}^{n}(x - x_i)$$

be a polynomial with n distinct roots x_i. Then

$$P''(x_i) = 2P'(x_i)\sum_{\substack{j=1\\ j\neq i}}^{n}\frac{1}{x_i - x_j}$$

We can apply this proposition to the Hermite polynomials. That the roots are isolated follows from the differential equation (13): At a double order zero, all derivatives of $H_n(x)$ would vanish.

If we evaluate the differential equation (13) of the Hermite polynomial at the root x_j, we get

$$H_n''(x_j) = 2x_jH_n'(x_j)$$

Using this in Proposition 5 we get

Corollary 1 *The zeroes x_i of the Hermite polynomial $H_n(x)$ satisfy*

$$x_i = \sum_{\substack{j=1\\ j\neq i}}^{n}\frac{1}{x_i - x_j} \tag{15}$$

We close this section with another little lemma:

Lemma 5 *Let x_0 be a zero of H_{n+1}. Then*

$$\frac{H_n'}{H_n}(x_0) = 2x_0$$

PROOF: By the recurrence relation (12) and the differential equation (14) we have

$$\begin{aligned} 0 &= H_{n+1}(x_0) \\ &= 2x_0 H_n(x_0) - 2nH_{n-1}(x_0) \\ &= 2x_0 H_n(x_0) - H_n'(x_0) \end{aligned}$$

Q.E.D.

6.3 Two Families of Balanced Configurations

In this section we will discuss two families of balanced configurations. We will call the first case the *definite* case, and the second case the *indefinite* case.

Proposition 6 (Definite Case) *Let $n \geq 1$ be an integer and let $\{x_i\}$ be the ordered set of roots of the Hermite polynomial H_n. Then $p_i = x_i$ form a balanced configuration for the charges $\epsilon_i = -1$.*

PROOF: This is a direct consequence of equation (15) and the definition.

For $n = 2$, one can check that the surface family obtained has all the properties of the twisted Karcher-Scherk surfaces ([4]). For $n = 3$ the surfaces were discussed by Hoffman, Karcher and Wohlrab as screw-motion invariant versions of singly periodic surfaces found by Fischer and Koch. The surfaces for larger n are new.

Proposition 7 (Indefinite Case) *Let $m \geq 0$ be an integer and let $n = 2m+1$. Let $\{p_i\}$ be the ordered set of zeroes of the two Hermite polynomials H_m and H_{m+1}. Then the p_i form a balanced configuration for the charges $\epsilon_i = -(-1)^i, \quad i = 1, \ldots, n$.*

PROOF: Denote by $x_i, \quad i = 1, \ldots, m+1$ the roots of H_{m+1}, and by $y_i, \quad i = 1, \ldots, m$ the roots of H_m. Observe that by equation 14 these are interlaced like

$$x_i < y_i < x_{i+1}$$

We need to distinguish two cases: First let $i = 2k$ be even so that $p_i = y_k$. Then we compute

$$\begin{aligned} p_i + \sum_{\substack{j=1 \\ j \neq i}}^{2m+1} \frac{\epsilon_j}{p_i - p_j} &= y_k + \sum_{j=1}^{m+1} \frac{1}{y_k - x_j} - \sum_{\substack{j=1 \\ j \neq k}}^{m} \frac{1}{y_k - y_j} \\ &= y_k + \left(\frac{d}{dx} \log H_{m+1}(x) \right)(y_k) - y_k \\ &= 0 \end{aligned}$$

where we have used equation (15) and the fact that $H'_{m+1}(x) = 2(m+1)H_m(x)$ so that y_k is a zero of $H'_{m+1}(x)$.

Now let $i = 2k-1$ be odd so that $p_i = x_k$. Then

$$\begin{aligned} p_i + \sum_{\substack{j=1 \\ j \neq i}}^{2m+1} \frac{\epsilon_j}{p_i - p_j} &= x_k + \sum_{\substack{j=1 \\ j \neq k}}^{m+1} \frac{1}{x_k - x_j} - \sum_{j=1}^{m} \frac{1}{x_k - y_j} \\ &= x_k + x_k - \left(\frac{d}{dx} \log H_m(x) \right)(x_k) \\ &= 0 \end{aligned}$$

with the help of Lemma 5.

Thus we obtain in both cases

$$p_i + \sum_{\substack{j=1 \\ j \neq i}}^{2m+1} \frac{\epsilon_j}{p_i - p_j}$$

and the claim follows. Q.E.D.

For $n = 3$, the surface family satisfies all properties of the screw motion invariant helicoids with handles discussed by [3, 10, 12] .The surface families for larger n are new.

Remark 1 *1. Are there other (real) balanced configurations? We believe that this is not the case, but don't have a complete proof of this.*

As an example, we can see that there are no balanced configurations with all charges $\epsilon_i = 1$ as follows: Evaluate

$$\begin{aligned}\sum_i p_i F_i &= \sum_i p_i^2 + \sum_{j\neq i} \frac{p_i}{p_i - p_j} \\ &= \sum_i p_i^2 + \sum_{i<j} 1 \\ &> 0\end{aligned}$$

Therefore, not all forces F_i can be zero.

2. *In particular we would like to know, whether there are other choices for the p_i with the same distribution of charges as in the indefinite case.*

3. *The situation changes when one looks at the complex version of the balance equations. These lead in the non-degenerate situation to more general screw-motion invariant embedded surfaces. Here we have found many exotic examples that most likely will defy any attempt of classification.*

6.4 Nondegeneracy in the definite case

In this section, we will prove that the family of balanced configurations is non-degenerate in the definite case, thus concluding the proof of part one of Theorem 2.

Fix a positive integer n and let x_k denote the zeroes of the Hermite polynomial H_n. Consider the matrix

$$H = (h_{ij}) = \begin{cases} \frac{1}{(x_i - x_j)^2} & \text{if } i \neq j \\ -\sum\limits_{\substack{k=1 \\ k\neq i}}^{n} \frac{1}{(x_i - x_k)^2} & \text{if } i = j \end{cases}$$

Observe that the non-degeneracy condition is equivalent to the condition that the matrix $1 - H$ is regular. We will compute all eigenvalues of H by finding a basis with respect to which H has upper triangular shape.

Definition 4 *Let x_i be the ordered zeroes of the n^{th} Hermite polynomial. Write $x = (x_i)$ and $x^s = (x_i^s)$. In particular, $x^0 = (1, 1, \ldots, 1)$.*

The following proposition is key main step of our computation:

Proposition 8 *$H \cdot x^s$ is a linear combination of $x^0, x^1, \ldots, x^s$, and the coefficient of x^s is $-s$.*

Corollary 2

$$\det(H - \lambda I) = (-1)^n \lambda \cdot (\lambda + 1) \cdot \ldots \cdot (\lambda + n - 1)$$

In particular, $\lambda = 1$ is not an eigenvalue of H, and the balanced configuration in the definite case is non-degenerate.

We begin the proof of Proposition 8 with a simple observation:

Lemma 6 *For all $s = 0, 1, 2, \ldots$*

$$\sum_{\substack{i=1 \\ i \neq k}}^{n} x_i^s = const - x_k^s$$

where const depends only on s and n but not on k. In other words, the left hand side of the equation is a polynomial in x_k of degree s with leading coefficient -1.

Proposition 9 *For all $s = 0, 1, 2 \ldots$*

$$\sum_{\substack{i=1 \\ i \neq k}}^{n} \frac{x_i^s}{x_k - x_i}$$

is a polynomial in x_k with leading coefficient $+1$ of degree $s + 1$.

PROOF: We will use the 'reproductive' property of the x_k from equation (15):

$$\sum_{\substack{i=1 \\ i \neq k}}^{n} \frac{1}{x_k - x_i} = x_k$$

Write

$$\begin{aligned}
\sum_{\substack{i=1\\ i\neq k}}^{n} \frac{x_i^s}{x_k - x_i} &= \sum_{\substack{i=1\\ i\neq k}}^{n} \frac{x_k^s}{x_k - x_i} - \frac{x_k^s - x_i^s}{x_k - x_i} \\
&= x_k^s \cdot \sum_{\substack{i=1\\ i\neq k}}^{n} \frac{1}{x_k - x_i} - \sum_{j=0}^{s-1} x_k^j \sum_{\substack{i=1\\ i\neq k}}^{n} x_i^{s-1-j} \\
&= -x_k^{s+1} - \sum_{j=0}^{s-1} x_k^j \sum_{\substack{i=1\\ i\neq k}}^{n} x_i^{s-1-j}
\end{aligned}$$

By Lemma 6, the last sum is a polynomial in x_k of degree at most $s-1$. Q.E.D.

Lemma 7 *We have $H \cdot x^0 = 0$ and $H \cdot x^1 = -x^1$*

PROOF: Only the second statement requires work:

$$\begin{aligned}
(H \cdot x^1)_k &= \sum_{i=1}^{n} h_{k,i} x_i \\
&= h_{k,k} x_k + \sum_{\substack{i=1\\ i\neq k}}^{n} h_{k,i} x_i \\
&= -\sum_{\substack{i=1\\ i\neq k}}^{n} \frac{x_k}{(x_k - x_i)^2} + \sum_{\substack{i=1\\ i\neq k}}^{n} \frac{x_i}{(x_k - x_i)^2} \\
&= -\sum_{\substack{i=1\\ i\neq k}}^{n} \frac{1}{x_k - x_i} \\
&= -x_k
\end{aligned}$$

Q.E.D.

PROOF: (Proposition 8)
Now let $r \geq 1$. By the same computation as above we get

$$(H \cdot x^r)_k = \sum_{\substack{i=1\\ i\neq k}}^{n} \frac{x_k^r - x_i^r}{x_k - x_i}$$

$$= \sum_{s=0}^{r-1} x_k^{r-s-1} \cdot \sum_{\substack{i=1 \\ i \neq k}}^{n} \frac{x_i^s}{x_k - x_i}$$

The summands $x_k^{r-s-1} \cdot \sum_{\substack{i=1 \\ i \neq k}}^{n} \frac{x_i^s}{x_k - x_i}$ are polynomials of degree r with leading coefficient -1, and there are r such summands. Q.E.D.

6.5 Non-degeneracy in the Indefinite Case

Let $x_1, \cdots, x_{m+1}$ be the zeroes of H_{m+1}, $y_1, \cdots, y_m$ be the zeroes of H_m. It will be convenient to arrange the configuration points p_i slightly differently here, namely so that

$$\epsilon_i = +1, \quad p_i = x_i, \quad 1 \leq i \leq m+1$$

$$\epsilon_{m+1+i} = -1, \quad p_{m+1+i} = y_i, \quad 1 \leq i \leq m \quad .$$

As we have seen in Proposition 7, this configuration satisfies

$$F_i = p_i + \sum_{j \neq i} \frac{\epsilon_j}{p_i - p_j} = 0 \quad .$$

Similar to the previous section we introduce the notation

$$x^r = (x_1^r, \cdots, x_{m+1}^r, 0, \cdots, 0)$$

$$y^r = (0, \cdots, 0, y_1^r, \cdots, y_m^r) \quad .$$

Then $\{x^0, \cdots, x^m, y^0, \cdots, y^{m-1}\}$ is a basis of $\mathbb{R}^n$, with $n = 2m+1$.

Lemma 8 *With respect to this basis, the matrix of the jacobian $\frac{\partial F_i}{\partial p_j}$ has the following form:*

$$M = \begin{pmatrix} A & B \\ C & D \end{pmatrix} \quad .$$

Let us say that a non-square matrix is triangular if it is zero below the 'diagonal' starting at the top left corner. Then A, B, C, D are triangular matrices, A and D are square of respective sizes $m+1$ and m. The coefficients on the "diagonals" are

$$A_{ii} = n + 1 - i$$

$$B_{ii} = -2(m + 1 - i)$$

$$C_{ii} = -2(m+1)$$

$$D_{ii} = n + 1 - i \quad .$$

Corollary 3 *We have*

$$\det(M) = \det(A')\det(D') = (m+1)(m!)^2 \qquad ,$$

and the balanced configuration is non-degenerate in the indefinite case.

PROOF: From Lemma 8 it is easy to compute the determinant of the jacobian: Perform the following row and columns operations on M:

$$R_{m+1+k} \to R_{m+1+k} + R_k, \quad 1 \le k \le m$$

and then

$$C_k \to C_k + C_{m+1+k}, \quad 1 \le k \le m \quad .$$

We obtain a matrix of the same form

$$M = \begin{pmatrix} A' & B' \\ C' & D' \end{pmatrix}$$

where C' is zero on the diagonal, and

$$A'_{ii} = i$$

$$D'_{ii} = i \quad .$$

Then, by performing more rows operations one can make C' zero without affecting the diagonals. So we obtain:

$$\det(M) = \det(A')\det(D') = (m+1)(m!)^2 \quad .$$

Q.E.D.

The proof of Lemma 8 follows the same method as the proof of Proposition 8, we just need a few more identities. Recall that the zeroes of the Hermite polynomials satisfy

$$\sum_{j \ne i} \frac{x_j^s}{x_i - x_j} = x_i^{s+1} + O(x_i^s) \quad .$$

The meaning of this equality is that the vector in $\mathbb{R}^{m+1}$ whose components are the left side, for $1 \le i \le m+1$, is equal to x^{s+1} plus a linear combination of x^r, $r \le s$. In the same way

$$\sum_{j \ne i} \frac{y_j^s}{y_i - y_j} = y_i^{s+1} + O(y_i^s) \quad .$$

We need identities for the quantities which involve both x and y.

Lemma 9

$$\sum_j \frac{y_j^s}{x_i - y_j} = 2x_i^{s+1} + O(x_i^{s-1})$$

$$\sum_j \frac{x_j^s}{y_i - x_j} = O(y_i^{s-1})$$

$$\sum_j \frac{1}{(x_i - y_j)^2} = 2m$$

$$\sum_j \frac{1}{(y_i - x_j)^2} = 2(m+1)$$

PROOF: Write

$$P = H_{m+1}, \quad Q = H_m \quad .$$

From Lemma 5 we get

$$\sum_j \frac{1}{x_i - y_j} = \frac{P''(x_i)}{P'(x_i)} = 2x_i \tag{16}$$

This proves the first formula in the case $s = 0$. The general case is obtained by induction as in the proof of Proposition 9.

By differentiating

$$\frac{Q'(z)}{Q(z)} = \sum_j \frac{1}{z - y_j}$$

and using the differential equation

$$Q'' = 2zQ' - 2mQ$$

we obtain

$$\sum_j \frac{-1}{(z - y_j)^2} = \frac{2zQ' - 2mQ}{Q} - \left(\frac{Q'}{Q}\right)^2$$

This gives

$$\sum_j \frac{-1}{(x_i - y_j)^2} = (2x_i)^2 - 2m - (2x_i)^2 = -2m \quad .$$

This proves the third equation. For the second equation at $s = 0$ use

$$\sum_j \frac{1}{z - x_j} = \frac{P'(z)}{P(z)} \tag{17}$$

and

$$P'(y_i) = 2(m+1)Q(y_i) = 0 \quad .$$

The general case follows again by induction. For the last equation, we differentiate equation (17):

$$\sum_j \frac{-1}{(z - x_j)^2} = \frac{P''}{P} - \left(\frac{P'}{P}\right)^2$$

Then $P'(y_i) = 0$ and using the differential equation for P,

$$P''(y_i) = -2(m+1)P(y_i)$$

which gives the result.

Now Lemma 8 can be proven as in the proof of Proposition 8, using the additional identities to deal with the mixed terms. Q.E.D.

References

[1] D. Hoffman, H. Karcher, and F. Wei. The genus one helicoid and the minimal surfaces that led to its discovery. In *Global Analysis and Modern Mathematics*. Publish or Perish Press, 1993. K. Uhlenbeck, editor, p. 119–170.

[2] D. Hoffman, H. Karcher, and F. Wei. The singly periodic genus-one helicoid. *Commentarii Math. Helv.*, pages 248–279, 1999.

[3] D. Hoffman and F. Wei. Deforming the periodic genus-one helicoid. *Experimental Mathematics*, 11(2):207–218, 2002.

[4] H. Karcher. Embedded minimal surfaces derived from Scherk's examples. *Manuscripta Math.*, 62:83–114, 1988.

[5] A. Lynker. Einfach periodische elliptische minimalflächen. Diplomarbeit Bonn, 1993.

[6] W. H. Meeks III and H. Rosenberg. The geometry of periodic minimal surfaces. *Comment. Math. Helvetici*, 68:538–578, 1993.

[7] G. Szego. *Orthogonal Polynomials*. Amer. Math. Soc., Providence, RI, 4 edition, 1975.

[8] M. Traizet. An embedded minimal surface with no symmetries. *J. Diff. Geometry*, 60:103–153, 2002.

[9] E. Koch W. Fischer. On 3-periodic minimal surfaces with non-cubic symmetry. *Zeitschrift für Kristallographie*, 183:129–152, 1988.

[10] M. Weber. The genus one helicoid is embedded. Habilitationsschrift Bonn, 2000.

[11] M. Weber. On Karcher's twisted saddle towers. In H. Karcher S. Hildebrandt, editor, *Geometric Analysis and Nonlinear Partial Differential Equations*. Springer, 2003.

[12] M. Weber, D. Hoffman, and M. Wolf. An embedded genus one helicoid. Preprint, 2004.